Reconfigurable Interfaces by Shape Change and Embedded Magnets

Himani Deshpande
hdeshpande11@tamu.edu
Computer Science and Engineering,
Texas A&M University
College Station, USA

Bo Han
bo.han@u.nus.edu
Industrial Design & Keio-NUS CUTE
Center, NUS
Singapore, Singapore

Kongpyung (Justin) Moon
jkpmoon@kaist.ac.kr
Industrial Design, KAIST
Daejeon, Republic of Korea

Andrea Bianchi
andrea@kaist.ac.kr
Industrial Design & School of
Computing, KAIST
Daejeon, Republic of Korea

Clement Zheng
clement.zheng@nus.edu.sg
Industrial Design & Keio-NUS CUTE
Center, NUS
Singapore, Singapore

Jeeeun Kim
jeeeun.kim@tamu.edu
Computer Science and Engineering,
Texas A& M University
College Station, USA
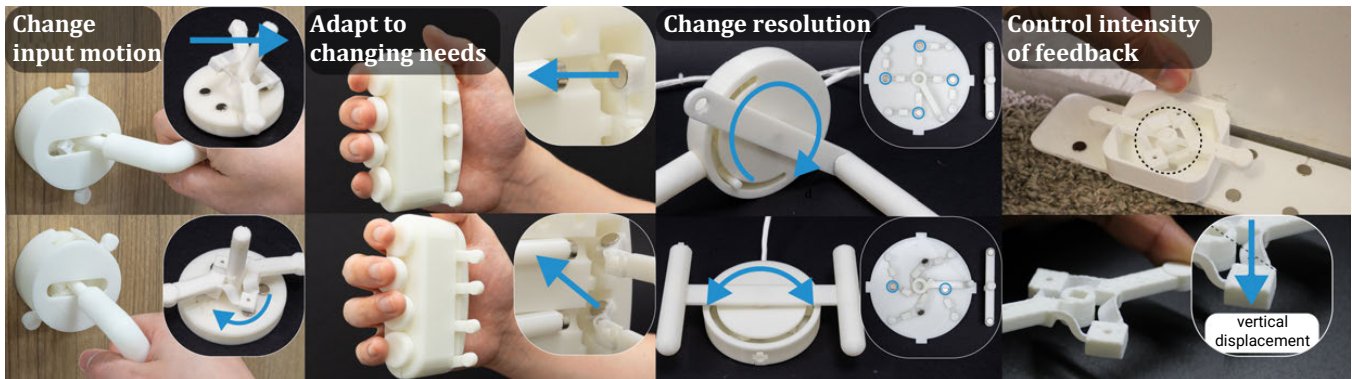
Figure 1: Our approach enables reconfiguration of physical interfaces in the form of input motions, adapting to changing needs, changing the resolution of the interface, and feedback intensity through shape change and displacement of embedded magnets.

ABSTRACT

Reconfigurable physical interfaces empower users to swiftly adapt to tailored design requirements or preferences. Shape-changing interfaces enable such reconfigurability, avoiding the cost of re-fabrication or part replacements. Nonetheless, reconfigurable interfaces are often bulky, expensive, or inaccessible. We propose a reversible shape-changing mechanism that enables reconfigurable 3D printed structures via translations and rotations of parts. We investigate fabrication techniques that enable reconfiguration using magnets and the thermoplasticity of heated polymer. Proposed interfaces achieve tunable haptic feedback and adjustment of different user affordances by reconfiguring input motions. The design space is demonstrated through applications in rehabilitation, embodied communication, accessibility, safety, and gaming.

CCS CONCEPTS

• **Human-centered computing → Human computer interaction (HCI)**.

KEYWORDS

Shape Change, Magnets, Fabrication

1 INTRODUCTION

In the rapidly evolving technological landscape, the demand for adaptable and personalized physical interfaces has grown substantially. While instances of modern digitization of input and output have displaced physical interfaces, they provide embodied interaction for non-visual information, multi-modal feedback for interactions in virtual reality (VR), and also partly contribute to the field of accessibility by simulating different human capabilities from what

has been impaired. Yet, traditional physical interfaces often require costly refabrication or part replacements to accommodate changing user preferences, and requirements [8, 25, 26], posing significant challenges in terms of cost, time, and sustainability as also noticed in prior works [31, 37]. Shape-changing interfaces offer an innovative solution to this problem by enabling mechanical reconfigurability without the need for extensive manufacturing processes. These include various physical reconfigurable devices, like input knobs [9], linear interfaces with rich I/O capabilites [19, 20], and pin-arrays [5]. Despite their potential, however, creating these interfaces remains challenging due to bulkiness, cost, and accessibility.

In response, previous works explored fabrication techniques that leverage the intrinsic material properties of heated 3D printed thermoplastic (e.g., PLA: PolyLactic Acid) [1, 29, 32, 33]—expansions and contractions due to external heat trigger [11], many equipped into novel actuators [6, 10, 11]. Despite these advantages, inaccuracies in shape-changing transformation, introduced by printing, strongly affect the usability and practical applicability. Our research explores a new fabrication technique that leverages magnets and a shape-memory thermoplastic to create a reversible shape-changing mechanism for reconfigurable interfaces. We use geometric control to constrain and guide the movements of heated thermoplastic along specified directions or rotations when force is applied, resulting in precise re-alignment of the 3D structure. As the embedded magnets move with the changed shape, the adjusted structure affects the magnetic field. Utilizing these capabilities, our interfaces can be used to deliver precise haptic feedback or can afford a variety of input motions. We delve into the behavior of these structures when exposed to heat in conjunction with the embedded magnets, introducing a comprehensive design space and applications that illustrate its practical usage in rehabilitation, communication, accessibility, safety, and gaming (Figure 1). In sum, we contribute:

- The design of a reconfigurable building block, with control parameters for a programmable displacement of embedded magnets.
- Principles for interaction reconfiguration using the relationship of shape change and embedded magnets
- Exemplary applications of reconfigurable interfaces demonstrating mechanisms in various design contexts.

2 BACKGROUND AND MOTIVATION

2.1 Multi-Use Physical Interfaces

Adjusting and customizing the interaction to suit individual preferences and needs are the major benefits of reconfigurability in physical interfaces. *KnobSlider* [9] introduces an interactive physical interface that mechanically changes its shape from rotary to linear slider to adapt to various software applications. *Button+* [27] is a context-aware interface that appears and disappears based on the user's situation to interact. Using a series of actuators to imbibe tunability into the interface, *InFORM* [5] introduces a pin-array display that changes its shape, providing various interaction affordances to the user with a single display. Similarly, *LineFORM* [20] uses several actuators in series to demonstrate how a chained linear interface can shape-change and adapt to interactions such as deformation, touch, and pinch. These works show how reconfigurability is vital to enrich user interaction in physical and virtual environments. However, these systems are often bulky due to embedded

actuators, and not accessible to lay users as they come with specific form-factor that do not fit bespoke interactive tangible interfaces.

We build upon the research in reconfiguring and customizing 3D-printed tangibles. For instance, *ReCompFig*[36] combines compliant mechanism and tensioning cables to develop a multi-modal kinematic mechanism capable of dynamically altering degrees of freedom. Enhancing and customizing existing physical objects, *Reprise* [3] creates 3D printed structures that allow users to modify everyday objects for a specific actions, such as adapting a wire cutter for single-finger operation. Davidoff et al. [4] and Li et al. [13] use 3D printed add-on mechanisms to actuate static objects such as adjusting the angle of a desk lamp [13], turning a car's climate control dial [4], or remotely silencing an alarm clock [24], showing the significance of customizing and reconfiguring tangible interfaces. However, a persistent challenge is the (re)fabrication of these mechanisms, which require external electro-mechanical actuators, microprocessors, and software coding.

2.2 Adaptive Interfaces by Shape-changing

Researchers have approached 3D printing shape-changing interfaces to achieve complex linear 3D structures from lines printed flat [32], transforming them by shifting directions of stimulus [28], and more. Combining shape-changeable objects with other materials such as TPU [1], carbon-composite PLA [18], and copper-sheet [23] activate transformation to obtain desired behaviors. For instance, chemically dissimilar bilayer structures release residual stress to bend a sample (e.g., [1]). *ShrinkCells* [18] and *Exoform* [23] use conductive materials either 3D printed or attached later on to control the activation time and to reconfigure the original shape per context, such as nailing a hook in and taking it out [18]. Although combining various materials in 3D printing allows for versatile activation of deformation, the generated shape changes are primarily limited to alterations in form factor [1, 18, 32]. Unfortunately, the force exerted by these shape shifts is insufficient to offer reconfigurability. To broaden the application of shape-changing objects in delivering haptic feedback and reshaping interaction affordances, we incorporate neodymium magnets within the 3D printed thermoplastic structures. This enhances the force feedback substantially, going beyond the limited residual force inherent in PLA filaments.

2.3 Magnets in Tangible Interfaces

Permanent magnets provide kinesthetic haptic feedback through pulling/ pushing forces arranged by polarity, position, and intensity. Embedded magnets can enable interactions with tabletop or portable displays [2, 14, 15, 34]. *Madget* [34] uses passive magnets in a physical interface to move, vibrate and power touch displays. Magnet-induced forces enable tangible blocks for interactive drawings [14] and identify different objects by their unique force [15]. Yet, these interactions require multiple physical interfaces with different topologies to attain more than one interaction (e.g., rotating and pushing), or changing the slider intervals for discreteness.

Beyond 2D interfaces, *MagnetIO* [16] introduced a soft stretchable magnetic patch to provide vibrotactile feedback when touched with a wearable device. *Mechamagnets* [31] introduced a tangible interface using permanent magnets with various topologies to provide kinesthetic feedback in various forms, such as linear, planar,

polar, radial, and angular motions. *Magneto-Haptics* [21], *Magnetips* [17], and *Omni* [12] have leveraged magnetism to enable both tracking and haptic feedback through embedding permanent magnets in tangible interfaces. Our work also provides kinesthetic feedback with permanent magnets in various orientations, positions, and intensities but most importantly, within a single 3D printed shape-changing interface that does not require external electromagnets for haptic feedback, yet still can afford different interaction styles (e.g., from rotation to linear), catering different extents of forces.

3 PRINCIPLES AND MODELING

Thermoplastic Behavior. Thermoplastics become flexible when heated, and respond to external activation and deactivation forces. As studied in many prior works, PLA also presents shape memory properties, by reverting to its original shape on being triggered after deformation. However, shape change is unpredictable in its repeatability if external deformation forces are applied by human intervention. Prior work [7, 22] has shown how geometric control can be leveraged for predictable and repeated shape change even when the shape changing forces are applied by humans. These works inspire use to control the geometry of our structures and constrain the areas of force application to ensure predictable repeatability.

Planning Predictable Deformations through Geometry Control. As introduced in prior work, square cells can shear, bend, and twist when aligned based on the angles of the opposing flexible hinges determining the in-plane or out-of-plane shape change [22]. The same principle applies to heat-based shape change by designing the geometry of a modular primitive. Intuitively, the malleability achieved after heating PLA is affected by the printed thickness and length. Longer and thinner parts heat up faster and bend easily due to the overall surface area heated directly, whereas, thicker parts take longer to heat throughout. Furthermore, the closer the length gets to the thickness, these parts become more difficult to bend. Using this logic, we devise the shape-change geometry with specific cells for force application, magnet housing, and hinge behavior.

3.1 Primitive Design

In/out-of-plane Displacement to Reconfigure Magnetic Fields. We investigate the in-plane and out-of-plane displacement of magnets embedded in the printed geometry by shape change. The geometry is designed to propagate applied force resulting in displacement of cells that house magnets in an elbow joint (Figure 2(a)).

- **Joints:** are the thinnest and longest parts of the geometry to be easily shape changed on application of heat and activation forces. They hence act as hinges for the entire structure.
- **Edge Cells:** are where manual activation force is applied. The force is applied along an arc connecting the cells. We design the edge cells to have a thickness to length ratio closer to 1, i.e. on application of heat and force, they will heat up but will not easily bend, propagating the force to the adjoining joints.
- **Magnet Cell:** is displaced in or out of its plane when activation force is applied to the edge cell. It is shaped as a cuboid with a hole where a magnet is inserted. It does not change its shape (thickness to length ratio close to 1). It moves in the 3D space by having forces propagated from edge cells through adjoining joints displacing the magnet cell and changing the magnetic field.
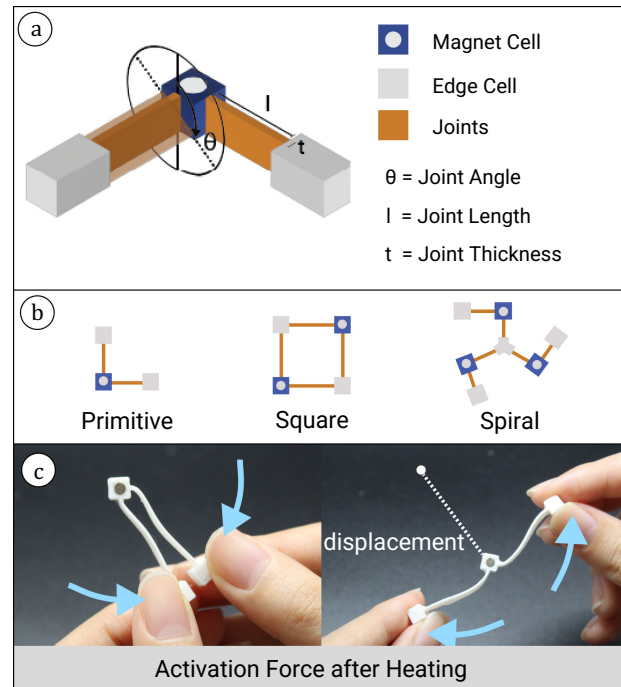

Figure 2: The structure of the shape-change geometry (a) is extracted from an elbow-joint building block. Geometric parameters program displacement of the magnet cell through shape change. We explore three topologies of the primitive (b). Activation forces (c) are applied at the edge cells to bring them closer, or pull them apart in the same plane.
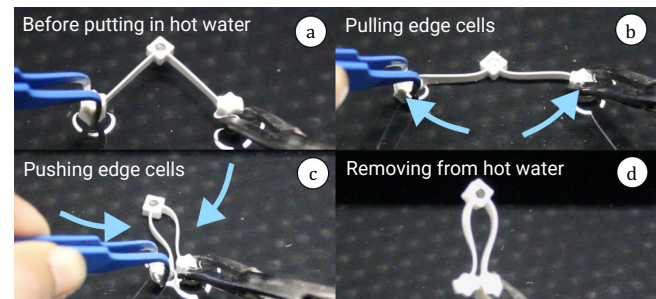
Figure 3: Process of triggering reconfiguration in hot water

Triggering Reconfiguration. We first heat the geometry using hot water, to apply heat uniformly as approached in many prior works. Note that in an end-user scenario, a more sophisticated embedded heating mechanism may be considered, including nichrome wires and/or conductive filaments for selective and sequential heating as needed. Once heated, pushing or pulling force is applied to the edge cells of the primitive geometry in a single arc connecting the two edge cells (Figure 2(c), Figure 3). This manual force is propagated through the joints to the magnet cell, and depending on the joint angle and length, displacement of the magnet cell from its original position can be predicted. We explore three topologies of the primitive i.e. the primitive, square, and the spiral (Figure 2(b)).

3.2 Displacement Modules and Parameters
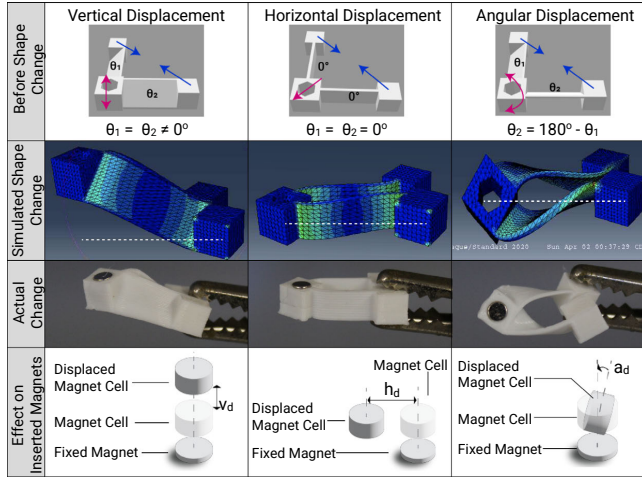
Figure 4: Vertical, Horizontal, and Angular displacement modules before/after shape change with their simulated models and the abstraction of the effect on embedded magnets.

Considering a fixed magnet directly below the magnet cell, displacing the magnet cell would change the attraction forces between the two magnets. If the magnet cell displaces beyond a certain distance or angle, the attraction forces will not affect the fixed magnet and the magnet cell, similar to "deactivating" the magnet cell. We can hence use the displacement modules (Figure 4) to affect the two magnets' magnetic field through predetermined shape change.

- **Vertical Displacement Module:** Vertical displacement (v_d) of the magnet cell is its displacement along the Z axis. Empirically, we found that the magnet cell is displaced vertically along the Z axis when both the adjoining joint angles are equal ($\theta_1 = \theta_2$).
- **Horizontal Displacement Module:** Horizontal displacement (h_d) of the magnet cell is seen when the joints are printed at 0°. This displacement is in the same plane as the magnet cell's previous position (X-Y plane). The direction of applied force to the edge cells determines the direction of the displacement.
- **Angular Displacement Module:** Angular displacement (a_d) of the magnet cell is the twisting of the magnet's orientation with respect to the X-Y plane. When the joint angles are opposite ($\theta_1 = 180° - \theta_2$), the magnet cell twists in an angular displacement.

3.3 Reconfiguration Supports for User Actions

While each topology (Figure 2 (b) summarizes a few of the possible topologies) provides reconfigurability, multiple edge cells can be hard to control through single input. A designer may want to hide the inner mechanism, but it would be imperative to provide access to reconfigure the mechanism quickly and easily. We explored additional supports for the mechanisms to shape change more than one magnet cell at once depending on the topology without knowing the inner working.

Push/Pull Edge Cells. For a simple primitve topology or even a square topology (Figure 2 (b)), an end user may have access to the edge cells to push them apart or closer together. However,

considerations need to be made when exposing multiple edge cells to the end user for displacing multiple magnet cells as follows.

Rotate Pole to Reshape. To make it easier to change shape with one swift action, rotating a central pole connecting the edge cells can move them closer or farther from each other. The center of shape change is preserved and there is no unnecessary displacement of the magnet cell (Figures 5 and 6). The addition of the central pole also enables simultaneous displacement of multiple magnet cells. For the square topology (Figure 2 (b)), we connect the edge cells to the center pole with thin connectors. We add stoppers at the base of the edge cells to prevent them from rotating. Hence, the rotation of the center pole blocks the edge cells, they move closer to the pole with the thin connectors twisting around (Figure 5). For the spiral topology (Figure 2 (b)), the central pole sits at the center. Here, two configurations are enabled, first, the central pole connects the edge cells similar to Figure 5 with stoppers. Second, we fix the outer edge cells of the spiral and rotate the central pole to move the magnet cells closer or further away from the center (Figure 6 (d)).

Pull Pole to Reshape. If the edge cells are fixed, a user can also pull the pole up, equivalent to pulling apart the edge cells but in a slanted plane (Figure 6(e)). The displacement can then be predicted with respect to the slanted plane. While more complicated topologies and placements of the central pole may be possible, these simpler topologies serve as building blocks.
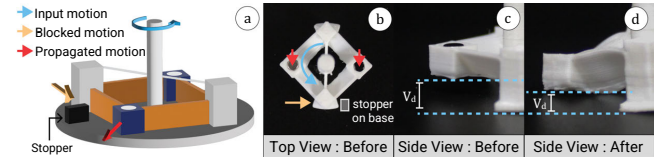
Figure 5: A square topology can utilize a center pole with thin connectors from the edge cells to the pole, and stoppers at the base (a,b,c). Rotating the center pole pushes the two edge cells together causing magnet cell displacement (d)
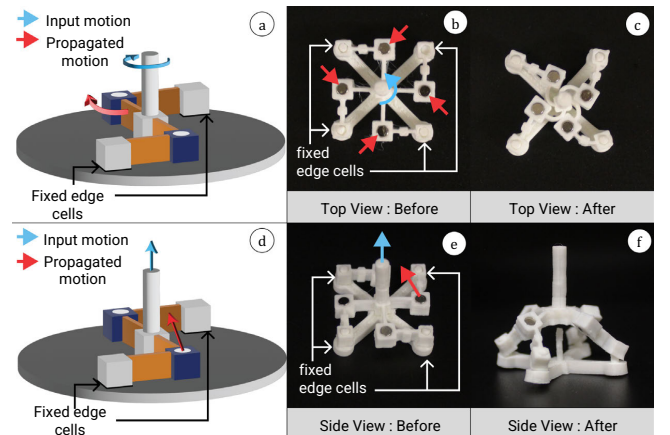
Figure 6: A spiral topology can utilize a center pole and stoppers, or even have its edge cells fixed (a,b). Rotating the pole results in magnets cells moving closer to the pole (c), and pulling up the pole (d,e) results in a dome shape (f)
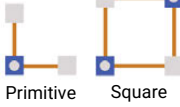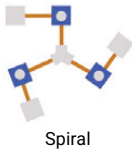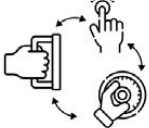
Figure 7: The design space describes the different options available to design reconfigurable interfaces as building blocks.

4 RECONFIGURABLE INTERFACES

Our design space helps users utilize the working principles in interaction design. It includes ways to control the displacement of embedded magnets through shape change, topology options, support for end users to reconfigure the interfaces easily, and the available reconfigurable interface properties as shown in Figure 7.

4.1 Properties and Applications

4.1.1 Haptic Feedback. By moving the magnet cells closer and further away from the fixed base magnets through displacement modules, the effect on magnetic forces results in changes in the haptic feedback received. For example, Figure 8 (a1,a2) shows the use of the square topology and vertical displacement to move the magnet cells closer to the ground. A slider mechanism (Figure 8 (b1,b2)) embeds this vertical displacement with metal nuts (or magnets) fixed in the base. Depending on the magnet cell's position closer or further away from the fixed nuts, the haptic feedback felt from the slider mechanism can be changed. For detailed evaluation of the felt haptic force, refer to Section 5.2.
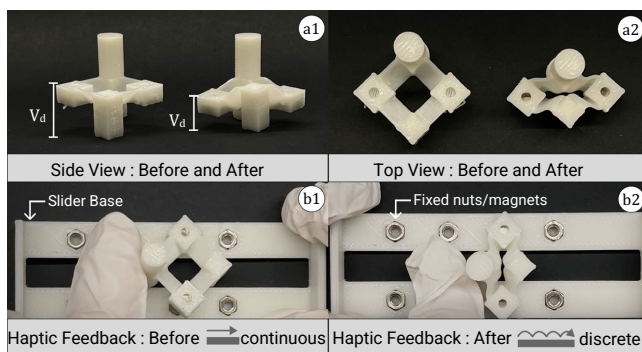

Figure 8: Vertical displacement of the magnet cells moves magnets closer to the slider base (a1,a2) increasing the feedback felt while moving the slider from a continuous motion with minimal feedback to discrete stepped feedback (b1,b2).

Application #1. Communicating Sliding Door. Haptic feedback can be a subtle technique of communicating information. For example, if a user is conducting an important zoom call in a common

workspace where multiple people are expected to show up, the user can adjust the haptic feedback of the sliding door indicating that the more force is needed to open the door, the more important it is to not make noise or disturb the user while accessing the common space. Similar to the slider in Figure 8, reconfiguring the sliding mechanism (Figure 9 (a)) to move the embedded magnets closer to the fixed magnets increases the force feedback (Figure 9 (b)).
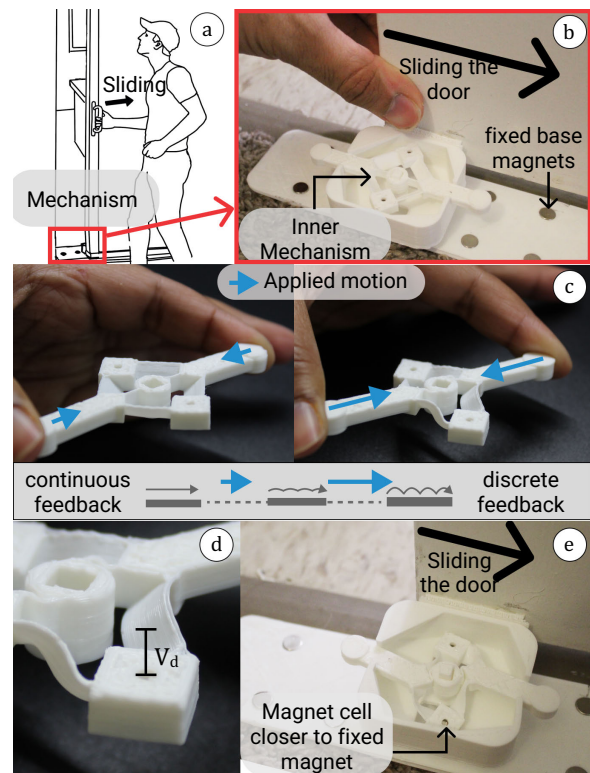

Figure 9: Reconfigurable haptic attachment is housed in a sliding door with fixed magnets on the floor (a,b). Reconfiguration increases the feedback discreteness (d) due to reduced distance between magnet cells and the fixed magnets (e,f).

Application #2. Physical Rehabilitation for Grip Strength.
A rehabilitation device with reconfigurable feedback can allow a
therapist to adjust force, adapting to changing user strength as pa-
tients regain grip strength. Figure 10 shows the rehabilitation device
where magnets are fixed to the buttons, and the shape changing
mechanisms behind the buttons house the responding magnets in a
primitive topology. The applied angular displacement module trig-
gers the displacement of the embedded magnets. In the initial state
aligned magnets repel strongly on button press. On undergoing
angular displacement, the force feedback is reduced.
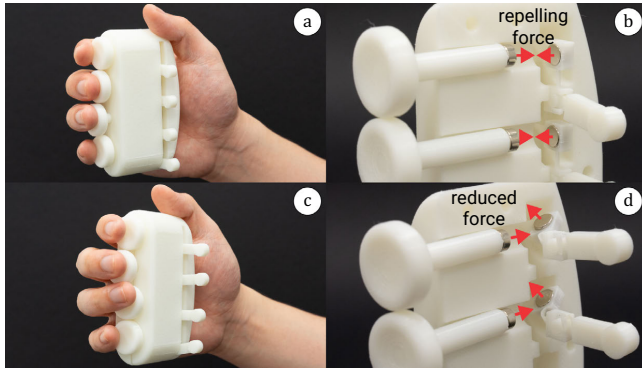
**Figure 10: Re-orienting the aligned magnets of a rehabilita-
tion device (a,b) reducing force feedback (c,d).**

Furthermore, we can design a rotary switch in a similar fashion
where the rotation of an added center pole can move the magnet
cells closer to the center, displacing them horizontally from the
base magnets (Figure 11). This mechanism uses the spiral topology,
and an added central pole as an end user support for reconfigura-
tion. Twisting the pole results in applying the displacement to the
magnets housed in the spiral, affecting the magnetic field.
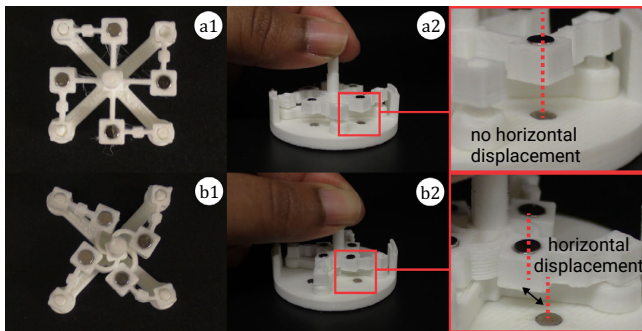
**Figure 11: Twisting the central pole of the spiral (a) moves
magnet cells close to the center in horizontal displacement (b)
with the fixed base magnets, and changes received feedback.**

We can also modify the number of steps felt (resolution) by acti-
vating and de-activating magnet cells through angular displacement
(Figure 12). When both magnet cells of a switch using square topol-
ogy are in play, a total of 10 steps are felt when using the switch
(Figure 12 (a1,a2)). However, on deactivating one of the magnet
cells, only 5 steps are felt (Figure 12 (b1,b2)).
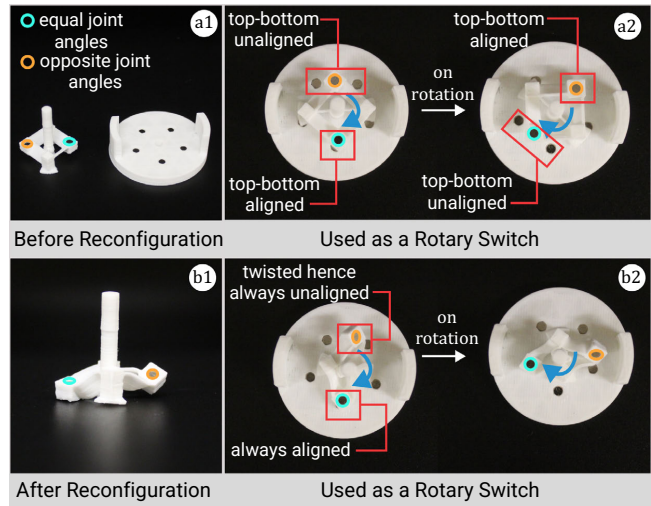
**Figure 12: The number of steps felt with two magnets in the
original state of the switch (a1,a2) is reduced by half when
the angular displacement module of the switch twists one
magnet cell, deactivating it (b1,b2).**

Application #3. Reconfigurable Game Controller. Utilizing the
reconfigurable haptic feedback to modify the number of felt steps
similar to Figure 12, we demonstrate a game controller design. For
a fishing game, the entire rotary motion is important with feedback
in the form of steps to simulate reeling-in fish using a fishing rod
(Figure 13 (a,b)). However, when playing a racing game, only two
steps of feedback for turning left and right may be needed. In this
case, we can utilize the angular displacement for two of the magnets
in the mechanism, reducing the steps felt from four to two (Figure
13 (c)). The controller can then be used as a steering wheel using
the same mechanism with a modified handle ((Figure 13 (d)).

**Figure 13: The fishing rod mechanism has four steps of dis-
crete feedback (a) felt when reeling-in fish in complete rota-
tions. Reconfiguration changes the number of steps to two
(c), felt during steering the controller to the left or right (d).**

4.1.2   Input Motion Affordances. While we focus on the displace-
ment of the magnet cell, the application of the shape change forces
can result in such an overall shape affording a new input motion.

For example, a square topology switch as show in Figure 14 (a) has space between the magnet cells and the ground such that it can pivot over a center pole for toggle motion. However, on application of vertical displacement we can move the magnet cells close to the ground constraining the toggle motion, making it more suitable for a rotary motion (Figure 14 (b)). Depending on the switch movement area and applied constraints such as a top cover, the rotary motion can also be turned to planar motion (Figure 14 (c)).
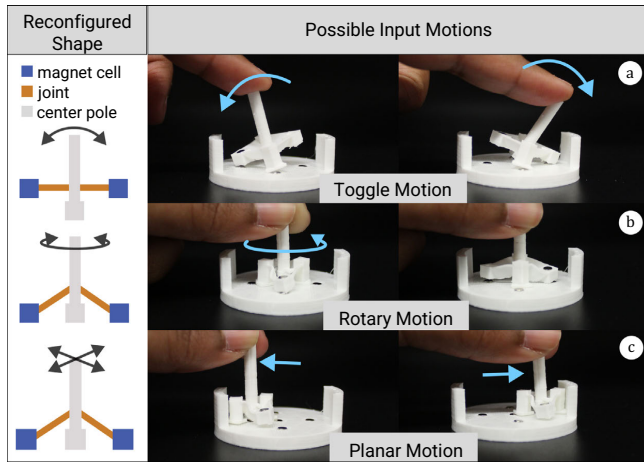

Figure 14: Reconfigured shape change enables reconfiguring toggle motion (a) to rotary (b) or planar motion (c).

Application #4. Dual-Motion Door-Knob. Most common door knobs require a rotation/twist input to open the door. However, if a user has wrist movement issues, they will have a hard time twisting the door knob. In such a case, a door knob that can be reconfigured to be toggled open can make the interaction easy for the user. Figure 15 shows a reconfigurable user door knob interaction from a rotation (Figure 15 (a,b)) to a toggle motion (Figure 15 (c,d)).
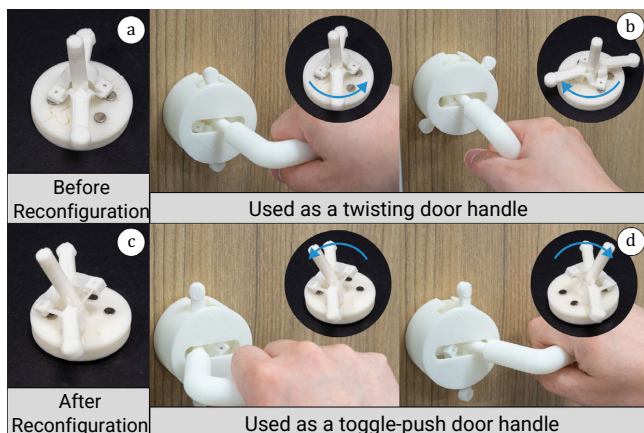

Figure 15: Reconfiguring twist motion (a,b) to toggle (c,d), afforded and constrained by shape change and magnets.

The manipulation of space around the mechanism can be utilized to reconfigure a push motion to a joystick motion (Figure 16).

Magnets are fixed in a cover. The space available inside the cover secures push motion for a button. The base of the mechanism is parallel to the cover top, and when pushed, it sits flush with the ground. The attraction to magnets in the cover prevents any toggle motions. However, pulling the center pole away from the base makes the mechanism occupy the space in the cover restricting the push motion. It can then be used as a joystick as the magnets cells are now reconfigured on a slant, and shifting the joystick enables specific magnets to align with the fixed magnets in the cover.
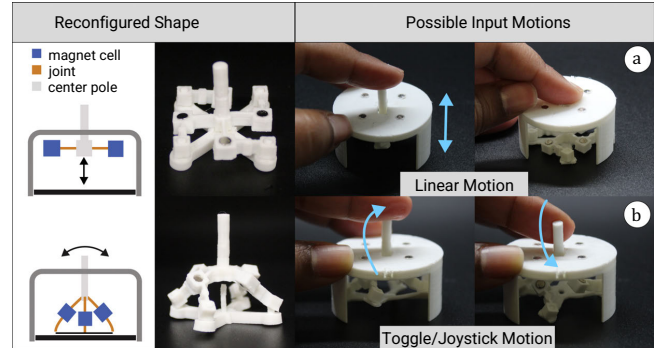
Figure 16: Push button motion (a) can be reconfigured to a toggle or joystick motion (b) by pulling up the center pole.

Application #5. Supporting Users via Affordances. Input motion reconfiguration can help when certain functions of the device need to be made inaccessible. For example, operating a toaster without knowing the extent of heat could be dangerous for a child or an elderly person with dementia. For users who require constrained use of the device, a simple push button can be pre-programmed with toasting settings (Figure 17(a)). However, a healthy adult may want full control over the temperature/timer settings, and reconfigure the push button to a four-way toggle switch to control temperature (Figure 17(b)) and time (Figure 17(c)).

Figure 17: Push interface can activate a pre-programmed set of steps for toasting (a). Reconfiguration of the mechanism can enable full control over temperature (b) and timer (c) settings through a four-way toggle motion.

4.2 Visual Cues to Assist Reconfiguration
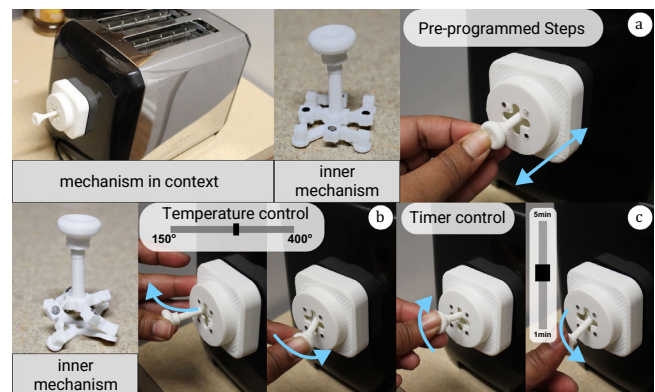
A designer might want the user to apply a specific level of displacement/force to the edge cells. For this, visual cues can be added on the fabricated widgets to aid users. For the three reconfiguration motions in the design space, the correlation of (1) rotating the center pole, (2) pulling it up, or (3) pushing or pulling the edge cells apart can be mapped onto a visual cue. We show an example of what such fabricated widgets might look like. Depending on the heating technique used, the materials of the widgets may be modified, for example, if the whole mechanism is to be put in hot water, the widget should be made of a material such as PolyEthylene Terephthalate Glycol (PETG , T_g = 85°C) or Acrylonitrile Butadiene Styrene(ABS, T_g = 105°C), with higher T_g (glass transition temperature) than PLA (60°C), so that the widget itself does not deform.
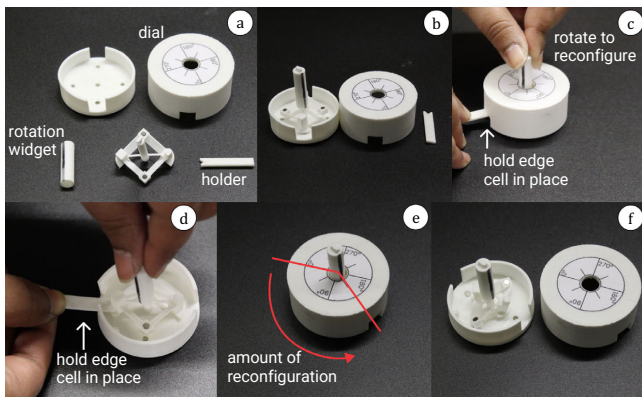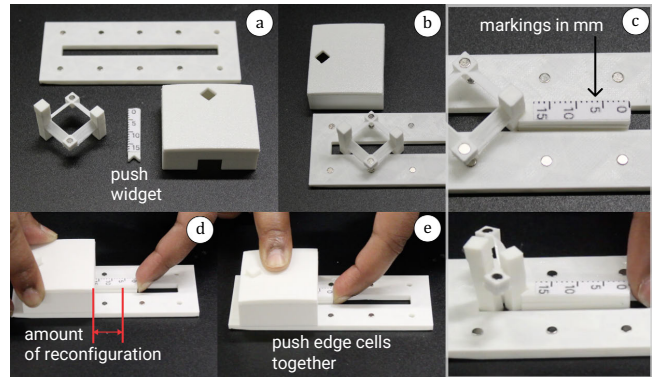

Figure 18: Using rotation widget for reconfiguration through rotation of center pole
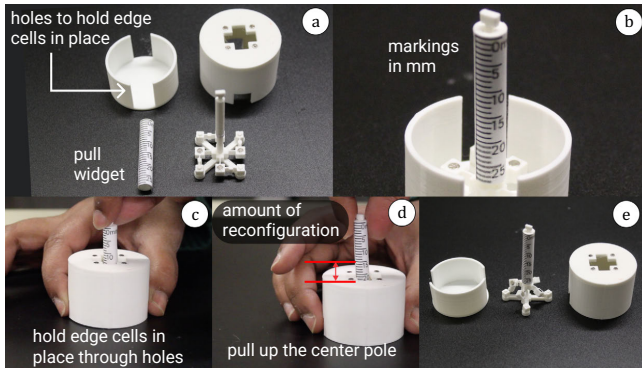
Figure 19: Using pull widget for reconfiguration through pulling up of center pole

For reconfiguration using rotation of the center pole on heating, a designer can use a dial based on the amount of reconfiguration required. In Figure 18, we used a dial with degrees showing the amount of rotation applied. A high-level representation such as icons of increasing haptic feedback, or low-mid-high strength can also be used to assist end-user perception of reconfiguration range.

Similarly, for the reconfiguration motion requiring the pulling up of the center pole after heating, the pole can have a widget cover indicating the length of the pole pulled up corresponding to the

Figure 20: Using push widget for reconfiguration through pushing edge cells together

expected deformation of the mechanism (Figure 19). Lastly, when pushing edge cells together for reconfiguration, a push widget that indicates how much the edge cell has been pushed in can give the user an idea of the expected feedback (Figure 20). These indicators can be ways of ensuring a specific type/amount of motion for reconfiguring a predefined amount of feedback. But, it is always possible for users to decide the amount based on personal preferences.

5 EVALUATION

### 5.1 Shape Change–Displacement Relationships

Related work has explored the control parameters of in/out-of-plane shape change to be hinge angles and their placements [22]. As we designed the geometry to work with heat-based shape change, and we are interested in displacement of the magnet cell through propagation of applied force, we first empirically validated that joint angles and lengths affect the magnet cell displacement.

To understand the relationships between joint angles and displacement, we printed a range of samples to gauge the relationships initially assessing parameter impact. We tested these samples by heating them in hot water and pushing the two edge cells together. We define joint angle θ as the angle made by the inner edge of the joint with respect to the vertical Z axis (refer Figure 2). From these samples, it was concluded that

- for movement of the magnet cell in the X-Y plane without any changes in Z axis, the joint angles must be set to 0°.
- for movement of the magnet cell in the Z axis without any changes in the X-Y plane, the joint angles must be equal
- to twist the magnet cell in the 3D space, the joint angles must be opposite i.e. subtracted from 180°(for e.g. 45°-135°.)

We also found that varying the joint length for the same joint angle resulted in different displacements. While the empirical evaluation unveiled a relationship between the joint angles and type of displacement, to further evaluate the effect of these parameters on the *extent* of magnet cell displacement, we conducted physics-based simulations measuring the displacements.

5.1.1 Apparatus and Procedure. Abaqus/CAE software enables Finite Element Modeling, visualization of the analyses, and simulating model states based on material, force, and environment settings. The software allows to test material-specific responses using PLA
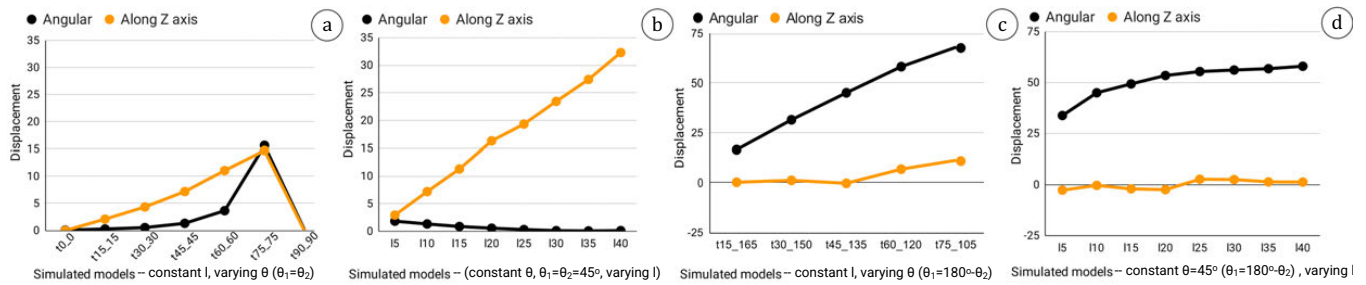
Figure 21: Displacements for (a) constant joint length (l) and increasing $\theta_1 = \theta_2$, (b) constant joint angle ($\theta_1 = \theta_2 = 45°$) and increasing joint lengths (l), (c) constant joint length (l) and increasing $\theta_1 = 180° - \theta_2$, (d) constant joint angle ($\theta_1 = 45°, \theta_2 = 135°$) and increasing joint lengths (l).

as input, and provided information about its characteristics and the environment. Given the ability to control the environment temperature and where the activation forces are applied, simulating the shape change using Abaqus gives close to real life results without human influence, and hence was chosen as a validation method. Tensile modulus was set to $3600MPa$ following the prior work [30] for PLA as our chosen shape memory material. Since the glass transition temperature (T_g) of PLA is generally between 60–65°C, the simulated temperature for triggering shape change was set to 80°C (> T_g). Since the amount of force applied by a human may vary, we simulate the displacement of the edge cells. For simulating the shape change, we fixed one edge cell and displace the other edge cell towards the fixed cell in the X-Y plane.
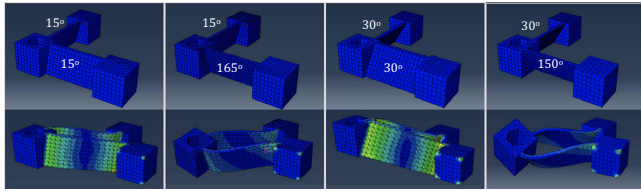
Figure 22: Representative simulations conducted in Abaqus

All angles between 0-180°at an interval of 15°were produced for testing. Based on the observation from preliminary testing, 12 samples were chosen for simulation (7 samples for equal angles, 5 samples for opposite angles) such that they covered all the combinations of the desired equal and opposite angles (45°-135°combination of angles is considered same as 135°-45°). The displacements of the magnet cells along X, Y, and Z axes, as well as the angular displacement were calculated by measuring the vector coordinates at the magnet cell before and after shape change.

In the second part of the simulations, we also tested the effect of various joint lengths on the displacement in two contexts, (1) where $\theta_1 = \theta_2 = 45°$ for displacement along Z axis, and (2) where $\theta_1 = 45°$ and $\theta_2 = 135°$ for angular displacement. Displacements for joint lengths $5 - 40mm$ with intervals of $5mm$ were tested. Figure 21 shows the results of the performed simulation tests. Figure 22 shows some representative simulated shape changed models.

5.1.2 Results. The evaluation experiments show the relationship of the joint angles and joint lengths of a primitive with the extent of displacement which we use in our application examples.

- When $\theta_1 = \theta_2 \neq 0°$,
  - v_d increases with increasing θ (without affecting a_d) where $\theta < 60°$ as a_d is prominent (> 5°) beyond $\theta = 60°$
  - v_d increases with increasing joint length(l)
- When $\theta_1 = 180° - \theta_2, \theta_1 < \theta_2$,
  - a_d increases with increasing θ_1(without affecting v_d) where $\theta < 60°$ as v_d is prominent beyond $\theta = 60°$

#1. Increasing equal joint angles show increasing Z axis displacement. Displacement along Z axis in samples with constant length increases with increase in joint angle ($\theta_1 = \theta_2$) returning to 0mm at $\theta = 90°$ (Figure 21(a)). However, we also see a certain amount of twisting or angular displacement as the angle increases. If we wish to control only the Z displacement, keeping the angular displacement to a minimum would be ideal i.e. in the range of 0-45°.

#2. For constant equal joint angles, Z axis displacement can be increased by increasing joint length (l). With $\theta_1 = \theta_2 = 45°$ with increasing joint lengths (l5-l40), the Z displacement increased linearly (Figure 21(b)). Hence, beyond the joint angle, we can increase the Z displacement further by increasing the joint length.

#3. Increasing opposite joint angles show increasing angular displacement Angular displacement increases with increase in θ_1 (Figure 21(c)). But beyond $\theta_1 = 45°$ ($\theta_2 = 180 - \theta_1 = 135°$), an increase in Z displacement is seen as well. Ideally if we only want to affect twisting, the Z displacement needs to be negligible. Hence, we recommend to use joint angles up to $\theta_1 = 45°$.

#4. For constant opposite joint angles, angular displacement reaches a maxima with increasing joint lengths (l). As seen from Figure 21(d), while we see negligible Z displacement for increasing joint lengths (l5-l40), the angular displacement does not increase linearly, saturating at about 62°.

5.2 Understanding the Effect on Magnets

To test the effect of spatial displacement of magnets within the magnet cells with respect to a fixed magnet directly below them, we measured the force-distance curves for different edge cell displacements. We used a dual-range force sensor coupled with a linear potentiometer to measure the distance between the magnet cell and the starting point. The force sensor pushes and pulls a 3D printed sample mechanism (square topology of the primitive geometry) hosting two magnets, along a rail with fixed magnets. Considering the maximum shape change as 0mm distance between
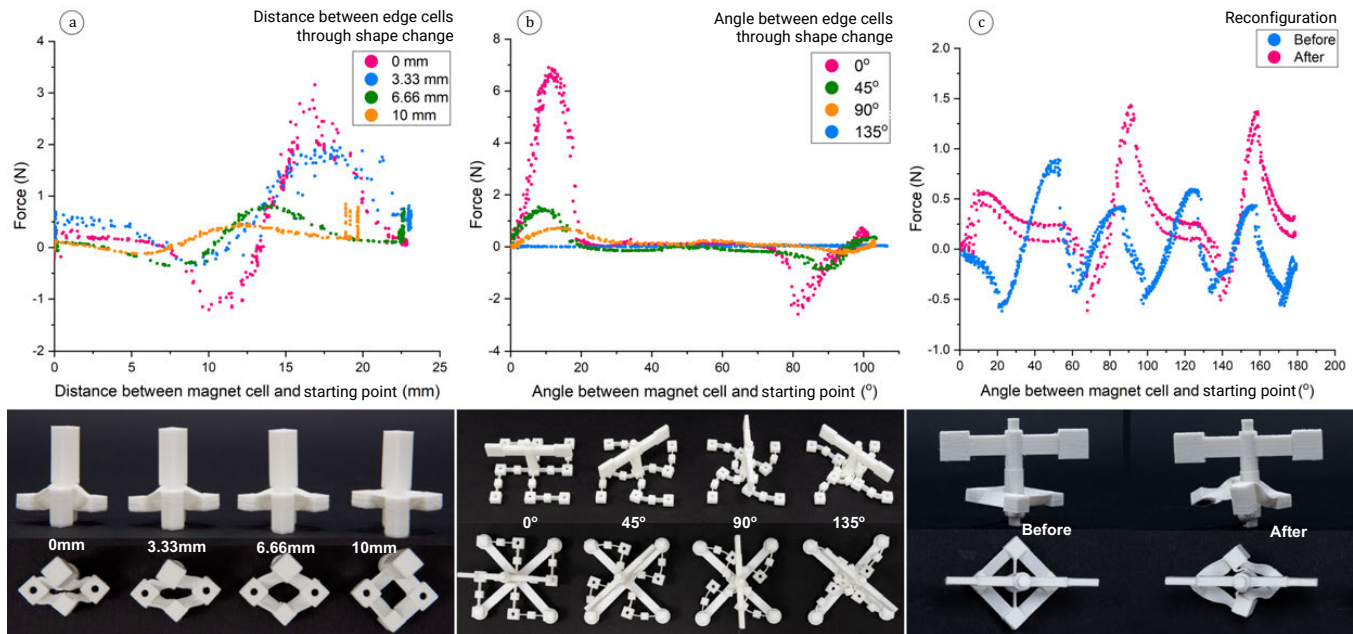
Figure 23: The force-distance/rotation curves obtained at various edge cell distances (a – top), reconfiguration angle (b – top) show that the force is proportional to the magnet cell's displacement. Changes in steps are felt before and after de-activating a magnet cell (c– top). (a,b,c – bottom) show the corresponding samples used for measurement.

edge cells, we tested distances of 3.33*mm*, 6.66*mm*, and 10*mm* (no shape change). Figure 23 (a) shows the tested samples, and the force-distance curves obtained. The Y axis shows the distance between the magnet cell and the starting point of the linear motion. The force-distance curve visualizes the haptic feedback during the relative movement of magnets. For our case of attracting magnets, when they approach each other, the pulling force increases (negative value) reaching the minimal value; when magnets move away from each other, the pulling force increases (positive value) until it reaches the maximal value. From the four force-distance curves of edge cell displacement, we observe a clear difference in maximum and minimum force values for each curve, where the 0*mm* displacement has the highest difference, and 10*mm* has the lowest.

We measured the force-rotation curve for different horizontal displacements based on the spiral topology. We used the same dual-range force sensor coupled with a rotary potentiometer. The force sensor pushed a 3D-printed spiral topology sample hosting four magnets, along a round base with four embedded magnets. Considering the maximum shape change to be 135°rotation of the center pole, we tested other angles of 90°, 45°, and 0°(no shape change) as shown in Figure 23(b). The force-rotation curve visualized the haptic feedback during the relative movement of magnets. We can observe a clear difference in both maximum and minimum force values for each curve, where the 0°sample has the highest pulling force during the rotation motion, while the 135°rotated sample has the smallest. The Y axis on the graph shows the angle between the magnet cell and the starting position.

We also measured the force-rotation curve for angular displacements based on the square topology, visualizing the steps felt (resolution) during the relative movement of magnets (Figure 23 (c)).

In the force curve of the switch where both magnet cells are in play, the peak and valley appear five times during the 180-degree rotation. In the force curve of the switch where one of the magnet cells is deactivated, two and a half times the peak and valley appear during the 180-degree rotation. The force–displacement/rotation curves showcase the different levels of resistance felt based on the applied amount of reconfiguration which can be utilized in the grip strengthener. The force is proportional to the displacement of the magnet cell from its original position. Hence, on scaling up the device geometry and using a proportionally larger magnet, the relationship between the feedback felt with the displacement of magnet cell from its original position should stay intact.

5.3 Repeatability: Recovery Testing

As the forces are applied manually and the recovery expected is through shape memory, we also test the devices' sustainment through multiple cycles of reconfiguration. As studied in the prior work, *"with decreasing deformation temperature and increasing recovery temperature, both the shape-recovery ratio and the maximum shape-recovery rate of the PLA samples increased"*, 90% recovery could be obtained [35]. Recovery ratio depends on the temperature at which the material is heated. As recovery attainable by 3D printed PLA has been previously investigated, we test on two sets of three primitive samples, at 2 joint lengths (15mm, 25mm), and 3 joint angle combinations (0°–0°, 45°–45°, and 45°–135°) to show that our mechanisms conform to the principle. Each primitive sample was heated, reconfigured by pushing edge cells together, cooled down, and then reheated for recovery for four cycles. As Figure 24 shows, the recovered shape is not exactly the same as the initial printed shape, however, the difference is minimal.
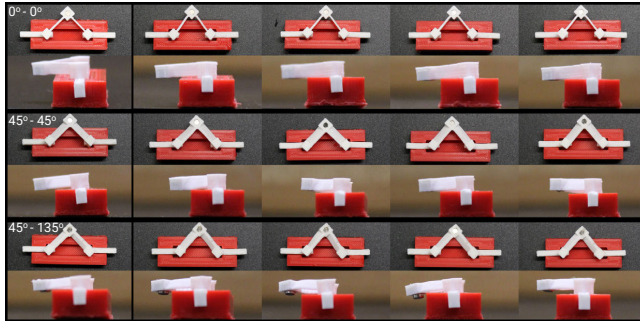
Figure 24: Recovery test over 4 cycles (first=initial) and recovery of primitive with 0°-0°, 45°-45°, and 45°- 135°joint angles.

6 DISCUSSION AND FUTURE WORK

6.1 Human Intervention in Reconfiguration

Our techniques require human intervention in the form of activation forces. We believe that this level of intervention may benefit humans by giving them the full power to customize the reconfiguration to their need. Reconfiguration is context and preference driven. Just as a musical instrument is tuned to the preference and requirement of a musician, or a replaceable shelf is moved by a shorter person to be able to reach the top, reconfiguration of interfaces is dependent on the human using them and that makes human intervention necessary to an extent. Our presented applications reiterate the contextual nature of reconfiguration where it may be needed based on humans' ability, need for communication in specific situations, safety, or simply a game's user experience.

6.2 Promoting Embodied Interaction

Recently, while digital interfaces are overshadowing tangible interfaces, we cannot discount the use of tangibility when it comes to multi-modal interactions. When users' visual capabilities are contextually impaired, for example, while driving, or being immersed in a VR environment, tangible and haptic interfaces provide the much needed information for both safety and embodied experience. We see the potential of haptic feedback and tactility in addressing accessibility concerns with visual or physical impairments (Figure 15), complementing digital interfaces, for rehabilitation devices (Figure 10), as well as for development of fine motor skills.

6.3 Other shape-changing mechanisms

We focus on manual shape change and recovery using shape memory. While programmable shape change allows programmed self-assembly when the printed artifact is triggered by heat, this technique utilizes the conflicting forces of shrinking caused by stresses released by the polymer in the direction of printed lines. Such artifacts cannot be "unshrunk" even after re-heating. Hence, the changes in the size would need to be accounted for in the design especially when embedding external objects such as magnets.

6.4 Further Evaluation and Design Assistance

We evaluated the relationship of joint angle and joint length with the displacement of the magnet cell. There are further geometric parameters such as the angle between joints and the joint thickness

contributing to the extent of displacement and speed of recovery. The relationship between different parameters can help in making design decisions for example, where higher displacement may be needed in constrained spatial conditions, or where vertical displacement might not be feasible and angular displacement might be the solution. The mechanisms created in this work mostly use $3mmx3mm$ or $6mmx3mm$ neodymium magnets. For higher magnetic forces and in larger devices, stronger magnets might be necessary. The relationship of these parameters can be utilized in an editor for assisting designers in creating similar mechanisms with input on the type of behavior expected.

7 CONCLUSION

We present reconfigurable interfaces, leveraging the shape-changing capabilities of 3D printed PLA and embedded magnets. Using displacement of embedded magnets when triggered by shape change, various applications demonstrate changing haptic feedback, and reconfigurable input motion to afford different interactions. We contribute techniques to create reconfigurable interfaces where added efforts in part replacement or refabrication can be circumvented.

ACKNOWLEDGMENTS

REFERENCES

[1] Byoungkwon An, Ye Tao, Jianzhe Gu, Tingyu Cheng, Xiang 'Anthony' Chen, Xiaoxiao Zhang, Wei Zhao, Youngwook Do, Shigeo Takahashi, Hsiang-Yun Wu, Teng Zhang, and Lining Yao. 2018. Thermorph: Democratizing 4D Printing of Self-Folding Materials and Interfaces. In *Proceedings of the 2018 CHI Conference on Human Factors in Computing Systems (CHI '18)*. Association for Computing Machinery, New York, NY, USA, 1–12. https://doi.org/10.1145/3173574.3173834

[2] Andrea Bianchi and Ian Oakley. 2013. Designing Tangible Magnetic Appcessories. In *Proceedings of the 7th International Conference on Tangible, Embedded and Embodied Interaction* (Barcelona, Spain) *(TEI '13)*. Association for Computing Machinery, New York, NY, USA, 255–258. https://doi.org/10.1145/2460625.2460667

[3] Xiang 'Anthony' Chen, Jeeeun Kim, Jennifer Mankoff, Tovi Grossman, Stelian Coros, and Scott E. Hudson. 2016. Reprise: A Design Tool for Specifying, Generating, and Customizing 3D Printable Adaptations on Everyday Objects. In *Proceedings of the 29th Annual Symposium on User Interface Software and Technology* (Tokyo, Japan) *(UIST '16)*. Association for Computing Machinery, New York, NY, USA, 29–39. https://doi.org/10.1145/2984511.2984512

[4] Scott Davidoff, Nicolas Villar, Alex S. Taylor, and Shahram Izadi. 2011. Mechanical Hijacking: How Robots Can Accelerate UbiComp Deployments. In *Proceedings of the 13th International Conference on Ubiquitous Computing* (Beijing, China) *(Ubi-Comp '11)*. Association for Computing Machinery, New York, NY, USA, 267–270. https://doi.org/10.1145/2030112.2030148

[5] Sean Follmer, Daniel Leithinger, Alex Olwal, Akimitsu Hogge, and Hiroshi Ishii. 2013. InFORM: Dynamic Physical Affordances and Constraints through Shape and Object Actuation. In *Proceedings of the 26th Annual ACM Symposium on User Interface Software and Technology* (St. Andrews, Scotland, United Kingdom) *(UIST '13)*. Association for Computing Machinery, New York, NY, USA, 417–426. https://doi.org/10.1145/2501988.2502032

[6] Freddie Hong, Connor Myant, and David E Boyle. 2021. Thermoformed Circuit Boards: Fabrication of Highly Conductive Freeform 3D Printed Circuit Boards with Heat Bending. In *Proceedings of the 2021 CHI Conference on Human Factors in Computing Systems* (Yokohama, Japan) *(CHI '21)*. Association for Computing Machinery, New York, NY, USA, Article 669, 10 pages. https://doi.org/10.1145/3411764.3445469

[7] Alexandra Ion, Johannes Frohnhofen, Ludwig Wall, Robert Kovacs, Mirela Alistar, Jack Lindsay, Pedro Lopes, Hsiang-Ting Chen, and Patrick Baudisch. 2016. Metamaterial Mechanisms. In *Proceedings of the 29th Annual Symposium on User Interface Software and Technology* (Tokyo, Japan) *(UIST '16)*. Association for Computing Machinery, New York, NY, USA, 529–539. https://doi.org/10.1145/2984511.2984540

[8] Mads Vedel Jensen, Jacob Buur, and Tom Djajadiningrat. 2005. Designing the User Actions in Tangible Interaction. In *Proceedings of the 4th Decennial Conference*

on Critical Computing: Between Sense and Sensibility (Aarhus, Denmark) *(CC '05)*. Association for Computing Machinery, New York, NY, USA, 9–18. https://doi.org/10.1145/1094562.1094565

[9] Hyunyoung Kim, Céline Coutrix, and Anne Roudaut. 2018. KnobSlider: Design of a Shape-Changing UI for Parameter Control. In *Proceedings of the 2018 CHI Conference on Human Factors in Computing Systems (CHI '18)*. Association for Computing Machinery, New York, NY, USA, 1–13. https://doi.org/10.1145/3173574.3173913

[10] Donghyeon Ko, Jee Bin Yim, Yujin Lee, Jaehoon Pyun, and Woohun Lee. 2021. Designing Metamaterial Cells to Enrich Thermoforming 3D Printed Object for Post-Print Modification. In *Proceedings of the 2021 CHI Conference on Human Factors in Computing Systems* (Yokohama, Japan) *(CHI '21)*. Association for Computing Machinery, New York, NY, USA, Article 671, 12 pages. https://doi.org/10.1145/3411764.3445229

[11] Xiao Kuang, Devin J. Roach, Jiangtao Wu, Craig M. Hamel, Zhen Ding, Tiejun Wang, Martin L. Dunn, and Hang Jerry Qi. 2019. Advances in 4D Printing: Materials and Applications. *Advanced Functional Materials* 29, 2 (2019), 1805290. https://doi.org/10.1002/adfm.201805290 arXiv:https://onlinelibrary.wiley.com/doi/pdf/10.1002/adfm.201805290

[12] Thomas Langerak, Juan José Zárate, David Lindlbauer, Christian Holz, and Otmar Hilliges. 2020. Omni: Volumetric Sensing and Actuation of Passive Magnetic Tools for Dynamic Haptic Feedback. In *Proceedings of the 33rd Annual ACM Symposium on User Interface Software and Technology* (Virtual Event, USA) *(UIST '20)*. Association for Computing Machinery, New York, NY, USA, 594–606. https://doi.org/10.1145/3379337.3415589

[13] Jiahao Li, Jeeeun Kim, and Xiang 'Anthony' Chen. 2019. Robiot: A Design Tool for Actuating Everyday Objects with Automatically Generated 3D Printable Mechanisms. In *Proceedings of the 32nd Annual ACM Symposium on User Interface Software and Technology* (New Orleans, LA, USA) *(UIST '19)*. Association for Computing Machinery, New York, NY, USA, 673–685. https://doi.org/10.1145/3332165.3347894

[14] Rong-Hao Liang, Liwei Chan, Hung-Yu Tseng, Han-Chih Kuo, Da-Yuan Huang, De-Nian Yang, and Bing-Yu Chen. 2014. GaussBricks: Magnetic Building Blocks for Constructive Tangible Interactions on Portable Displays. In *Proceedings of the SIGCHI Conference on Human Factors in Computing Systems* (Toronto, Ontario, Canada) *(CHI '14)*. Association for Computing Machinery, New York, NY, USA, 3153–3162. https://doi.org/10.1145/2556288.2557105

[15] Rong-Hao Liang, Han-Chih Kuo, Liwei Chan, De-Nian Yang, and Bing-Yu Chen. 2014. GaussStones: Shielded Magnetic Tangibles for Multi-Token Interactions on Portable Displays. In *Proceedings of the 27th Annual ACM Symposium on User Interface Software and Technology* (Honolulu, Hawaii, USA) *(UIST '14)*. Association for Computing Machinery, New York, NY, USA, 365–372. https://doi.org/10.1145/2642918.2647384

[16] Alex Mazursky, Shan-Yuan Teng, Romain Nith, and Pedro Lopes. 2021. MagnetIO: Passive yet Interactive Soft Haptic Patches Anywhere. In *Proceedings of the 2021 CHI Conference on Human Factors in Computing Systems (CHI '21)*. Association for Computing Machinery, New York, NY, USA, Article 213, 15 pages. https://doi.org/10.1145/3411764.3445543

[17] Jess McIntosh, Paul Strohmeier, Jarrod Knibbe, Sebastian Boring, and Kasper Hornbæk. 2019. Magnetips: Combining Fingertip Tracking and Haptic Feedback for Around-Device Interaction. In *Proceedings of the 2019 CHI Conference on Human Factors in Computing Systems* (Glasgow, Scotland Uk) *(CHI '19)*. Association for Computing Machinery, New York, NY, USA, 1–12. https://doi.org/10.1145/3290605.3300638

[18] Kongpyung (Justin) Moon, Haeun Lee, Jeeeun Kim, and Andrea Bianchi. 2022. ShrinkCells: Localized and Sequential Shape-Changing Actuation of 3D-Printed Objects via Selective Heating. In *Proceedings of the 35th Annual ACM Symposium on User Interface Software and Technology* (Bend, OR, USA) *(UIST '22)*. Association for Computing Machinery, New York, NY, USA, Article 86, 12 pages. https://doi.org/10.1145/3526113.3545670

[19] Ken Nakagaki, Artem Dementyev, Sean Follmer, Joseph A. Paradiso, and Hiroshi Ishii. 2016. ChainFORM: A Linear Integrated Modular Hardware System for Shape Changing Interfaces. In *Proceedings of the 29th Annual Symposium on User Interface Software and Technology* (Tokyo, Japan) *(UIST '16)*. Association for Computing Machinery, New York, NY, USA, 87–96. https://doi.org/10.1145/2984511.2984587

[20] Ken Nakagaki, Sean Follmer, and Hiroshi Ishii. 2015. LineFORM: Actuated Curve Interfaces for Display, Interaction, and Constraint. In *Proceedings of the 28th Annual ACM Symposium on User Interface Software & Technology* (Charlotte, NC, USA) *(UIST '15)*. Association for Computing Machinery, New York, NY, USA, 333–339. https://doi.org/10.1145/2807442.2807452

[21] Masa Ogata. 2018. Magneto-Haptics: Embedding Magnetic Force Feedback for Physical Interactions. In *Proceedings of the 31st Annual ACM Symposium on User Interface Software and Technology* (Berlin, Germany) *(UIST '18)*. Association for Computing Machinery, New York, NY, USA, 737–743. https://doi.org/10.1145/3242587.3242615

[22] Jifei Ou, Zhao Ma, Jannik Peters, Sen Dai, Nikolaos Vlavianos, and Hiroshi Ishii. 2018. KinetiX-designing auxetic-inspired deformable material structures.

[23] *Computers & Graphics* 75 (2018), 72–81.

[23] Fang Qin, Huai-Yu Cheng, Rachel Sneeringer, Maria Vlachostergiou, Sampada Acharya, Haolin Liu, Carmel Majidi, Mohammad Islam, and Lining Yao. 2021. ExoForm: Shape Memory and Self-Fusing Semi-Rigid Wearables. In *Extended Abstracts of the 2021 CHI Conference on Human Factors in Computing Systems (CHI EA '21)*. Association for Computing Machinery, New York, NY, USA, Article 249, 8 pages. https://doi.org/10.1145/3411763.3451818

[24] Raf Ramakers, Fraser Anderson, Tovi Grossman, and George Fitzmaurice. 2016. RetroFab: A Design Tool for Retrofitting Physical Interfaces Using Actuators, Sensors and 3D Printing. In *Proceedings of the 2016 CHI Conference on Human Factors in Computing Systems* (San Jose, California, USA) *(CHI '16)*. Association for Computing Machinery, New York, NY, USA, 409–419. https://doi.org/10.1145/2858036.2858485

[25] Joon Gi Shin, Doheon Kim, Chaehan So, and Daniel Saakes. 2020. Body Follows Eye: Unobtrusive Posture Manipulation Through a Dynamic Content Position in Virtual Reality. In *Proceedings of the 2020 CHI Conference on Human Factors in Computing Systems* (Honolulu, HI, USA) *(CHI '20)*. Association for Computing Machinery, New York, NY, USA, 1–14. https://doi.org/10.1145/3313831.3376794

[26] Joon-Gi Shin, Eiji Onchi, Maria Jose Reyes, Junbong Song, Uichin Lee, Seung-Hee Lee, and Daniel Saakes. 2019. Slow Robots for Unobtrusive Posture Correction. In *Proceedings of the 2019 CHI Conference on Human Factors in Computing Systems* (Glasgow, Scotland Uk) *(CHI '19)*. Association for Computing Machinery, New York, NY, USA, 1–10. https://doi.org/10.1145/3290605.3300843

[27] Jihoon Suh, Wooshik Kim, and Andrea Bianchi. 2017. Button+: Supporting User and Context Aware Interaction through Shape-Changing Interfaces. In *Proceedings of the Eleventh International Conference on Tangible, Embedded, and Embodied Interaction* (Yokohama, Japan) *(TEI '17)*. Association for Computing Machinery, New York, NY, USA, 261–268. https://doi.org/10.1145/3024969.3024980

[28] Lingyun Sun, Jiaji Li, Yu Chen, Yue Yang, Ye Tao, Guanyun Wang, and Lining Yao. 2020. 4DTexture: A Shape-Changing Fabrication Method for 3D Surfaces with Texture. In *Extended Abstracts of the 2020 CHI Conference on Human Factors in Computing Systems* (Honolulu, HI, USA) *(CHI EA '20)*. Association for Computing Machinery, New York, NY, USA, 1–7. https://doi.org/10.1145/3334480.3383053

[29] Lingyun Sun, Yue Yang, Yu Chen, Jiaji Li, Danli Luo, Haolin Liu, Lining Yao, Ye Tao, and Guanyun Wang. 2021. ShrinCage: 4D Printing Accessories That Self-Adapt. In *Proceedings of the 2021 CHI Conference on Human Factors in Computing Systems* (Yokohama, Japan) *(CHI '21)*. Association for Computing Machinery, New York, NY, USA, Article 433, 12 pages. https://doi.org/10.1145/3411764.3445220

[30] J Antonio Travieso-Rodriguez, Ramon Jerez-Mesa, Jordi Llumà, Oriol Traver-Ramos, Giovanni Gomez-Gras, and Joan Josep Roa Rovira. 2019. Mechanical properties of 3D-printing polylactic acid parts subjected to bending stress and fatigue testing. *Materials* 12, 23 (2019), 3859.

[31] Guanyun Wang, Ye Tao, Ozguc Bertug Capunaman, Humphrey Yang, and Lining Yao. 2019. A-line: 4D Printing Morphing Linear Composite Structures. In *Proceedings of the 2019 CHI Conference on Human Factors in Computing Systems* (Glasgow, Scotland Uk) *(CHI '19)*. Association for Computing Machinery, New York, NY, USA, 1–12. https://doi.org/10.1145/3290605.3300656

[32] Guanyun Wang, Ye Tao, Ozguc Bertug Capunaman, Humphrey Yang, and Lining Yao. 2019. A-line: 4D Printing Morphing Linear Composite Structures. In *Proceedings of the 2019 CHI Conference on Human Factors in Computing Systems* (Glasgow, Scotland Uk) *(CHI '19)*. Association for Computing Machinery, New York, NY, USA, 1–12. https://doi.org/10.1145/3290605.3300656

[33] Guanyun Wang, Humphrey Yang, Zeyu Yan, Nurcan Gecer Ulu, Ye Tao, Jianzhe Gu, Levent Burak Kara, and Lining Yao. 2018. 4DMesh: 4D Printing Morphing Non-Developable Mesh Surfaces. In *Proceedings of the 31st Annual ACM Symposium on User Interface Software and Technology* (Berlin, Germany) *(UIST '18)*. Association for Computing Machinery, New York, NY, USA, 623–635. https://doi.org/10.1145/3242587.3242625

[34] Malte Weiss, Florian Schwarz, Simon Jakubowski, and Jan Borchers. 2010. Madgets: Actuating Widgets on Interactive Tabletops. In *Proceedings of the 23rd Annual ACM Symposium on User Interface Software and Technology* (New York, New York, USA) *(UIST '10)*. Association for Computing Machinery, New York, NY, USA, 293–302. https://doi.org/10.1145/1866029.1866075

[35] Wenzheng Wu, Wenli Ye, Zichao Wu, Peng Geng, Yulei Wang, and Ji Zhao. 2017. Influence of Layer Thickness, Raster Angle, Deformation Temperature and Recovery Temperature on the Shape-Memory Effect of 3D-Printed Polylactic Acid Samples. *Materials* 10, 8 (Aug. 2017), 970. https://doi.org/10.3390/ma10080970

[36] Humphrey Yang, Tate Johnson, Ke Zhong, Dinesh Patel, Gina Olson, Carmel Majidi, Mohammad Islam, and Lining Yao. 2022. ReCompFig: Designing Dynamically Reconfigurable Kinematic Devices Using Compliant Mechanisms and Tensioning Cables. In *Proceedings of the 2022 CHI Conference on Human Factors in Computing Systems (CHI '22)*. Association for Computing Machinery, New York, NY, USA, Article 170, 14 pages. https://doi.org/10.1145/3491102.3502065

[37] Clement Zheng, Zhen Zhou Yong, Hongnan Lin, HyunJoo Oh, and Ching Chiuan Yen. 2022. Shape-Haptics: Planar & Passive Force Feedback Mechanisms for Physical Interfaces. In *Proceedings of the 2022 CHI Conference on Human Factors in Computing Systems (CHI '22)*. Association for Computing Machinery, New York, NY, USA, Article 171, 15 pages. https://doi.org/10.1145/3491102.3501829